Internet Journal of Society for Social Management Systems Vol.11 Issue 2 sms17-1329
ISSN: 2432-552X
ORIGINAL ARTICLE

A Study on the Risk Assessment of Emergency Supplies Transportation Routes Considering Scenario Earthquakes

Kazuaki Torisawa[1], Harumi Yashiro[2], Sei'ichiro Fukushima[3*], Satoshi Kina[4]

[1] Kajima Technical Research Institute
2-19-1 Tobitakyu, Chofu-shi, Tokyo, 182-0036, JAPAN

[2] National Defense Academy of Japan
1-10-20 Hashirimizu, Yokosuka-shi, Kanagawa, 239-8686, JAPAN

[3] RKK Consulting
1-4-33-1421 Shiohama, Koto-ku, Tokyo, 135-0043, JAPAN

[4] Yokohama National University
79-1 Tokiwadai, Hodogaya-ku, Yokohama-shi, Kanagawa 240-8501, JAPAN

[*]E-mail: fukushima@rkk-c.co.jp

***Abstract*:** When large-scale earthquake disasters occur in the metropolitan area, it is difficult to procure the necessary supplies within the affected area for many victims, so it is very important to secure access from outside of the affected area. In this research, in order to contribute to the rational choice of emergency transportation route in the Tokyo metropolitan area, we proposed a risk assessment and comparison method for transport route candidates, and showed specific examples of evaluation. As a result of this study, it was shown that it is possible to provide information that contributes to the rational choice of emergency supplies transportation route by multiplying the risk of target route against several assumed earthquakes.

Keywords: emergency supply, transport route, scenario earthquake, damage to roads, liquefaction, road blockade, damage to bridge

1. Introduction

When large-scale earthquake disasters occur in the metropolitan area, it is difficult to procure the necessary supplies within the affected area for many victims, so it is very important to secure access from outside of the affected area. The government is planning to secure an emergency transport route for severe high-impact earthquake (inland earthquake of magnitude seven class) in the capital city, but in that study only the earthquake beneath the southern city center is assumed and other earthquakes are not taken into direct consideration. In addition, road damage estimation is done to examine the plan to open the road after the earthquake, but risk

Received: 2017.08.08 / Accepted: 2018.02.07
Internet Journal of Society for Social Management Systems Published Date: 2018.07.10

comparison between routes is not done.

In this research, in order to contribute to the rational choice of emergency transportation route in the Tokyo metropolitan area, we propose a risk assessment and comparison method for transport route candidates, and showed specific examples of evaluation.

2. Condition setting for Risk Assessment

2.1 Scenario earthquakes

Four earthquakes immediately below the capital assumed by the Central Disaster Prevention Council are selected as scenario earthquakes. The location of the earthquakes is shown in Fig.1 with other earthquakes employed for damage estimation by the Central Disaster Prevention Council.

Bold red lines in the Fig. 1 are the scenario earthquakes whose macro characteristics are summarized in Table 1.

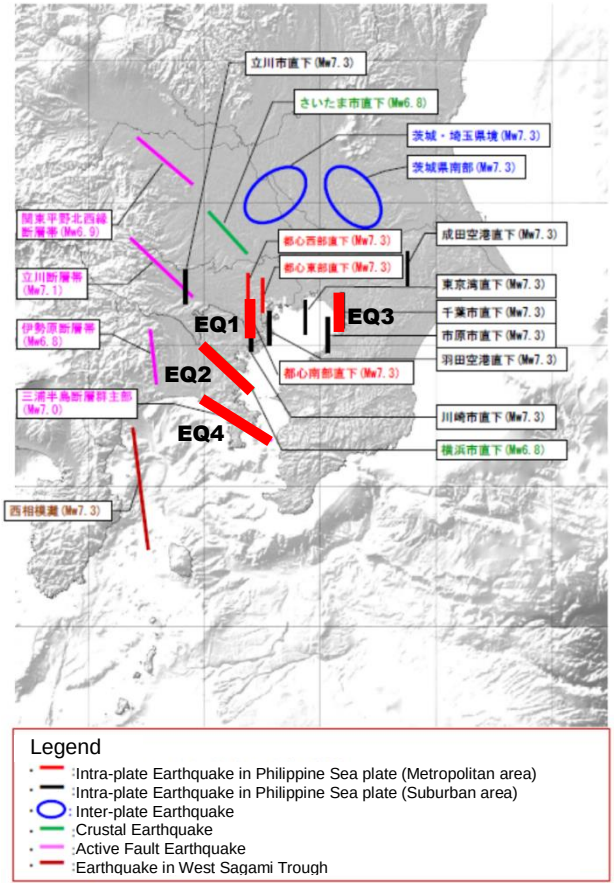

Fig.1 Scenario earthquakes

Table 1 Parameters for scenario earthquakes

	EQ1	EQ2	EQ3	EQ4
EQ Type	Intra-Pl.	Crustal	Intra-Pl.	Crustal
Longitude	139.72°	139.70°	140.11°	139.77°
Latitude	35.60°	35.35°	35.48°	35.178°
Depth	26.8 km	6 km	29.7 km	5 km
Length	28.1 km	23.0 km	28.1 km	28.0 km
Width	32.1 km	12.0 km	32.1 km	14.0 km
Strike	0°	315°	0°	300°
Dip	90°	60°	90°	45°
MW	7.3	6.8	7.3	7.0

2.2 Transport routes

Six transport routes are selected in the analysis as shown in Fig.2, in which numbers in the figure denote the routes described in Table 2.

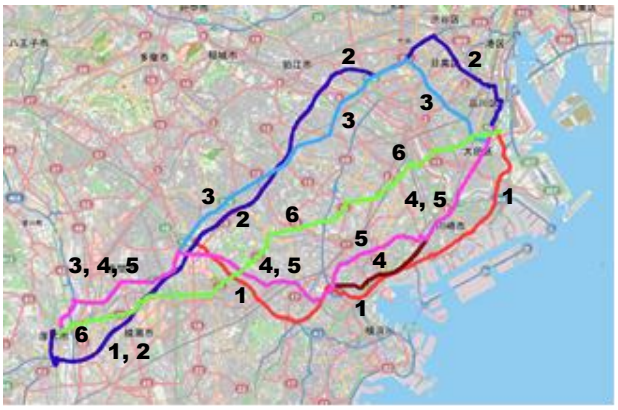

Fig.2 Candidates of transport routes

Table 2 Features of transport routes

Route	Total Length (km)	Number of 1-km meshes crossed	Number of 250-m meshes crossed
1	57.716	72	282
2	57.402	75	281
3	49.934	62	249
4	48.585	57	233
5	49.580	56	237
6	43.040	48	195

2.3 Risk items

In the analysis the following phenomena; damage to roads, liquefaction, road blockade by collapsed buildings and damage to bridge, are selected as risks to be estimated. It is noted that the phenomena above

have strong correlation with one another since they are common cause failure due to ground shaking.

3. Risk analysis

3.1 Procedure of risk analysis

Fig. 3 shows the flowchart of risk analysis employed in the research.

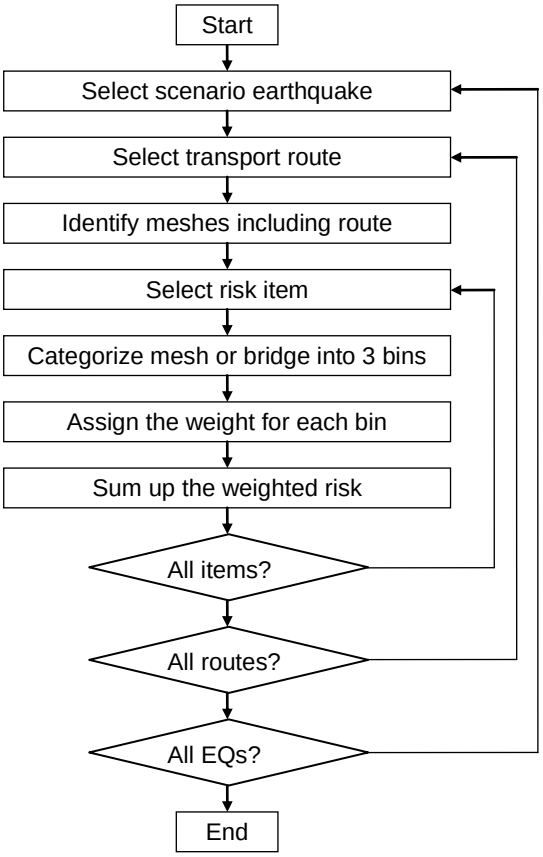

Fig. 3 Flowchart of risk analysis

3.2 Result of risk analysis

3.2.1 Damage to roads

Damage to roads is categorized into 3 bins using the ground motion intensity of the mesh along the route of concern. In the analysis, categorization is done as follows.

- Class A: JMA Intensity is 6+ or greater
- Class B: JMA Intensity is 6-
- Class C: JMA Intensity is 5+ or smaller

Distribution of ground motion intensity is shown in Fig. 4.

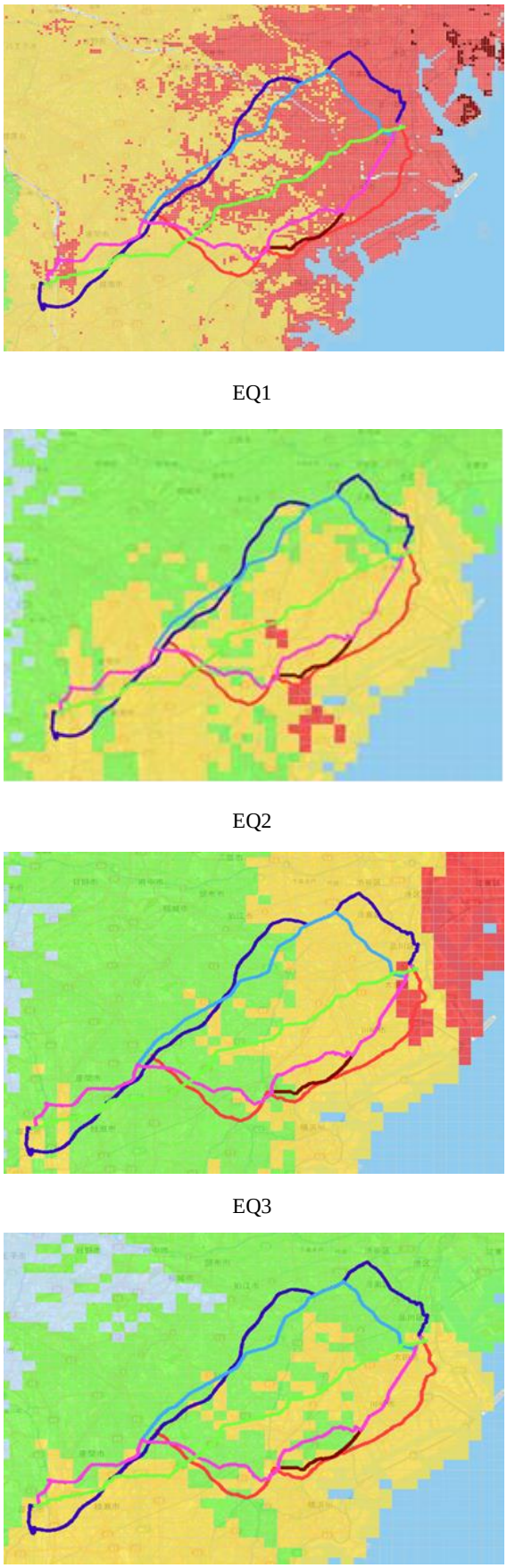

EQ1

EQ2

EQ3

EQ4

Fig. 4 Distribution of ground motion intensity

The numbers of mesh along the route for each class are summarized in Table 3, where the values are arranged in the order of class A, B and C.

Table 3 Number of mesh for each class
(Damage to roads)

Route	Scenario Earthquake			
	EQ1	EQ2	EQ3	EQ4
1	116/165/1	1/66/5	5/31/36	0/55/17
2	106/175/0	0/33/42	0/37/38	0/24/51
3	111/138/0	0/23/39	0/25/37	0/8/54
4	115/118/0	1/46/10	2/25/30	0/30/27
5	100/137/0	0/46/10	2/25/29	0/24/32
6	115/80/0	1/43/4	0/26/22	0/32/16

3.2.2 Liquefaction

Liquefaction is categorized into 3 bins based on the liquefaction probability in case of earthquake as follows.

- Class A: Probability is 10% or greater
- Class B: Probability is 5-10%
- Class C: Probability is less than 5%

The liquefaction probability is given by the JMA Intensity and micro-topography as shown in Fig. 5.

Distribution of liquefaction probability is shown in Fig. 6.

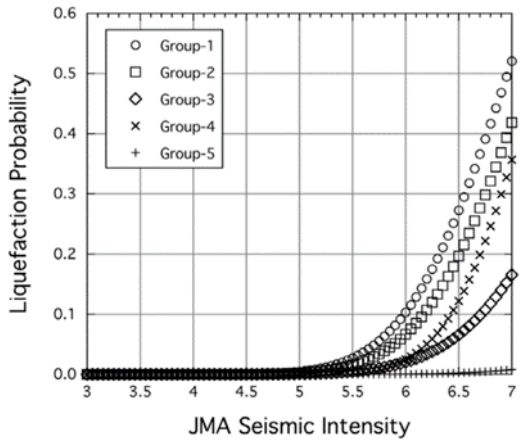

Fig. 5 Relationship between ground motion intensity and liquefaction probability

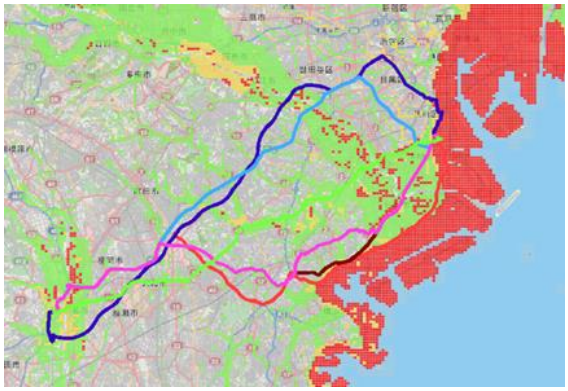

EQ1

EQ2

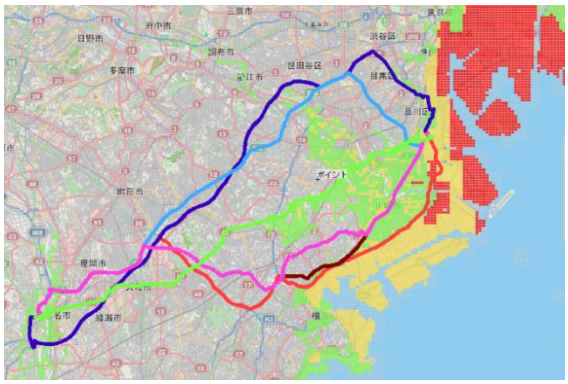

EQ3

EQ4

Fig. 6 Distribution of liquefaction probability

The numbers of mesh along the route for each class are summarized in Table 4, where the values are arranged in the order of class A, B and C.

Table 4 Number of mesh for each class
(Liquefaction)

Route	Scenario Earthquake			
	EQ1	EQ2	EQ3	EQ4
1	61/15/206	3/27/123	4/53/95	0/4/148
2	19/13/248	0/0/133	0/9/120	0/1/116
3	9/13/225	0/0/88	0/7/73	0/8/78
4	13/26/191	0/4/148	0/14/129	0/0/151
5	12/11/211	0/0/124	0/11/105	0/0/124
6	16/6/173	0/0/118	0/8/108	0/0/118

3.2.3 Road blockade

Road blockade is categorized into 3 bins based on the blockade number, which is obtained as the product of road length in a mesh of concern and road blockade rate.

- Class A: Number of blockade is 2.5 or more
- Class B: Number of blockade is 1.0 to 2.5
- Class C: Number of blockade is 1.0 or less

The road blockade rate is given as shown in Fig. 7 that were obtained from the past damage data.

Distribution of road blockade is shown in Fig. 8.

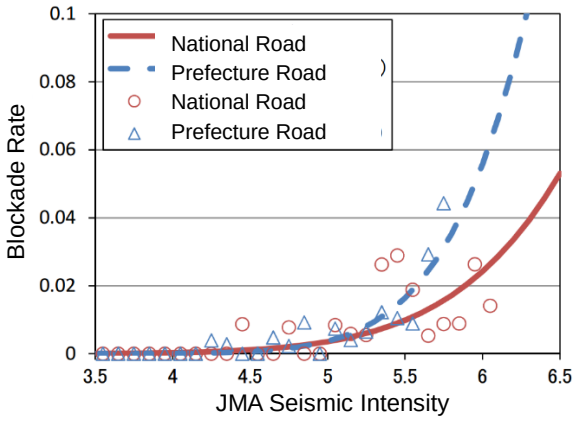

Fig. 7 Relationship between ground motion intensity and blockade rate
(number of blockade per unit length)

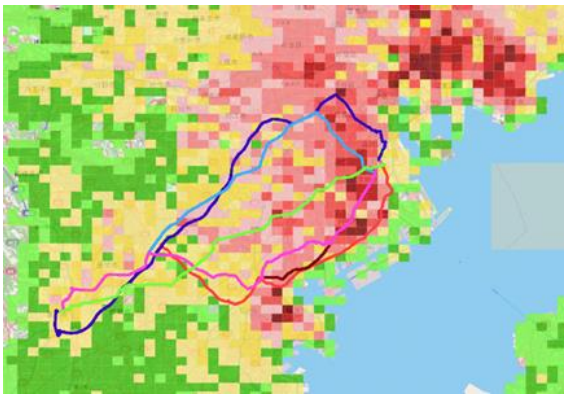

EQ1

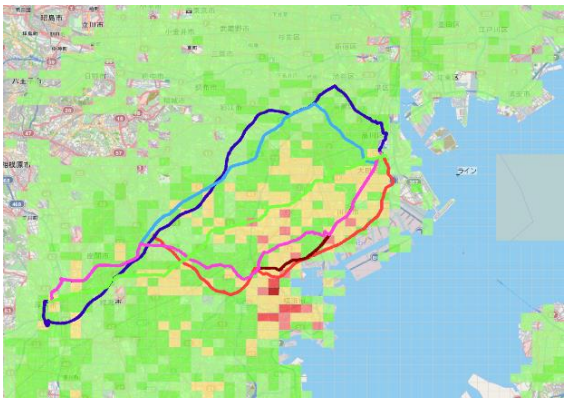

EQ2

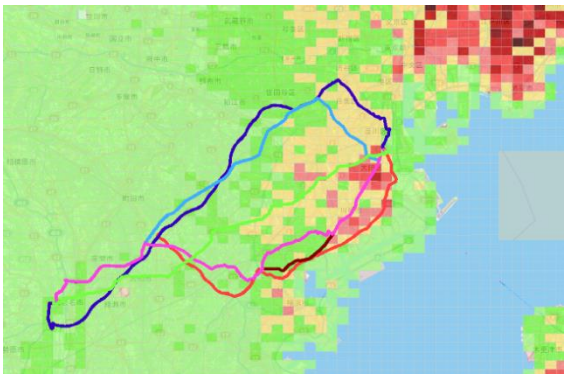

EQ3

EQ4

Fig. 8 Distribution of road blockade

The numbers of mesh along the route for each class are summarized in Table 5, where the values are arranged in the order of class A, B and C.

Table 5 Number of mesh for each class (Road blockade)

Route	Scenario Earthquake			
	EQ1	EQ2	EQ3	EQ4
1	0/3/19	0/1/21	0/0/22	0/0/22
2	0/12/5	0/0/17	0/1/16	0/0/17
3	5/40/17	0/0/62	0/1/61	0/0/62
4	5/30/21	0/5/51	0/10/46	0/0/56
5	5/32/20	0/3/54	0/9/48	0/0/57
6	4/29/15	0/4/44	0/4/44	0/0/48

3.2.4 Damage to bridge

Damage to bridge is categorized into 3 bins as follows.

- Class A: Collapse or severe
- Class B: Moderate
- Class C: Slight

The locations of bridges are shown in Fig. 9. Being different from other risk items, damages to bridge are calculated bridge by bridge using the Table 6 and are combined using following equation,

$$P_j = 1 - \prod_{i=1}^{n} (1 - p_{ij}),$$

where suffixes i and j denote bridge and damage class, respectively.

Fig. 9 Location of bridges along the routes

Table 6 Damage rate of bridge

Intensity	Damage Class		
	A	B	C
6+	0.024	0.086	0.462
6-	0.010	0.045	0.358
5+	0.003	0.014	0.262
5-	0.000	0.007	0.162

The damage rates P_j of each route are summarized in Table 7, where the values are arranged in the order of class A, B and C.

Table 7 Damage rate of route by bridge damage for each class

Route	Scenario Earthquake			
	EQ1	EQ2	EQ3	EQ4
1	0.193 0.556 0.997	0.096 0.369 0.988	0.058 0.241 0.930	0.089 0.348 0.986
2	0.132 0.418 0.981	0.055 0.228 0.940	0.048 0.202 0.932	0.034 0.150 0.910
3	0.153 0.468 0.990	0.057 0.238 0.956	0.031 0.135 0.923	0.044 0.188 0.942
4	0.153 0.468 0.990	0.064 0.262 0.962	0.044 0.188 0.942	0.057 0.238 0.956
5	0.153 0.468 0.990	0.064 0.262 0.962	0.044 0.188 0.942	0.057 0.238 0.956
6	0.141 0.444 0.988	0.077 0.308 0.971	0.057 0.238 0.956	0.077 0.308 0.971

4. Comparison of routes based on the risk

4.1 Procedure of comparison

In this study, the total risk of the route is given by the following equation,

$$R_i = \sum_{k=1}^{4} r_{ik},$$

where suffixes i and k denote route and risk item, respectively. Variable r_{ik} is the relative weakness that

is obtained as the weighted sum of the individual relative weakness r_{ijk}. Namely, r_{ik} is given by the following equation,

$$r_{ik} = \sum_{j=1}^{3} (w_j \cdot r_{ijk}),$$

where suffixes j denotes damage class. Variable w_j is the weight that is 5 for Class A, 4 for Class B and 3 for Class C, respectively. Variable r_{ijk} is obtained from the risk from Tables 3, 4, 5 and 7 by normalizing by the maximum value.

4.2 Prioritization of Transport routes

4.2.1 In case of EQ1

Variable r_{ik} and the sum R_i in case of EQ1 is summarized in Table 8, in which R.D., Liq, R.B. and Bridge denote road damage, liquefaction, road blockade and bridge damage, respectively.

The radar chart of relative weakness is shown in Fig. 10, by which the characteristics of each route are made clear. For example, the risk of blockade in routes 1 and 2 are considerably small comparing to other routes. In other routes, route 6 possess the small risks in 4 risk items so that route 6 gives the smallest risk as shown in Table 8 followed by the route 2 with second smallest risk.

From the viewpoint of risk, route 6 is the best according to the Table 8, followed by route 2.

Table 8 Relative weakness (EQ1)

Route	r_{ik}				R_i
	R.D.	Liq.	R.B.	Bridge	
1	1.000	1.000	0.292	1.000	3.292
2	0.990	0.906	0.288	0.854	3.038
3	0.891	0.785	1.000	0.907	3.583
4	0.842	0.755	0.881	0.907	3.358
5	0.843	0.750	0.903	0.907	3.408
6	0.720	0.634	0.767	0.881	3.002

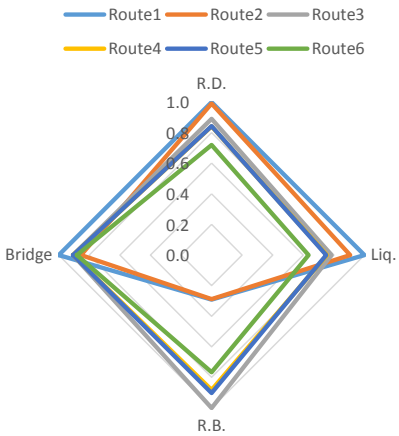

Fig. 10 Radar chart of relative weakness (EQ1)

4.2.2 In case of EQ2

The relative weaknesses are summarized in Table 9 and Fig. 11 as in case of EQ2. Similar tendency as in case of EQ1 case is observed though the smallest risk is appeared in route 2. Namely route 2 is the best followed by route 6.

Table 9 Relative weakness (EQ2)

Route	r_{ik}				R_i
	R.D.	Liq.	R.B.	Bridge	
1	1.000	1.000	0.360	1.000	3.360
2	0.908	0.811	0.290	0.863	2.872
3	0.736	0.537	1.000	0.874	3.147
4	0.771	0.935	0.930	0.897	3.533
5	0.754	0.756	0.935	0.897	3.342
6	0.665	0.720	0.796	0.940	3.121

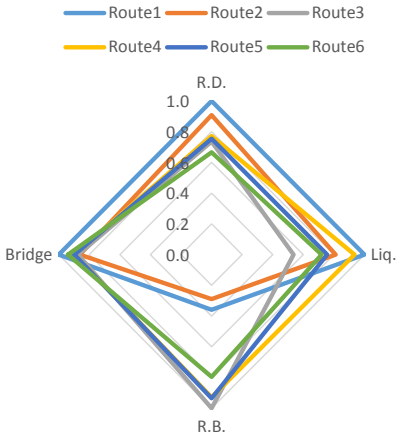

Fig. 11 Radar chart of relative weakness (EQ2)

4.2.3 In case of EQ3

The relative weaknesses are summarized in Table 10 and Fig. 12 as in case of EQ3. Similar tendency as in case of EQ1 case is observed though the smallest risk is appeared in route 2. Namely route 2 is the best followed by route 6.

Table 10 Relative weakness (EQ3)

Route	r_{ik}				R_i
	R.D.	Liq.	R.B.	Bridge	
1	0.986	1.000	0.353	1.000	3.339
2	1.000	0.766	0.294	0.822	2.882
3	0.805	0.478	1.000	0.741	3.025
4	0.763	0.857	0.952	0.812	3.384
5	0.754	0.694	0.963	0.812	3.223
6	0.649	0.689	0.791	0.878	3.007

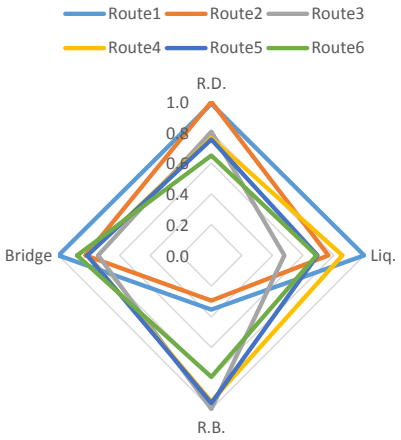

Fig. 12 Radar chart of relative weakness (EQ3)

4.2.4 In case of EQ4

The relative weaknesses are summarized in Table 11 and Fig. 13 as in case of EQ3. Similar tendency as in case of EQ1 case is observed though the smallest risk is appeared in route 2. Namely route 2 is the best followed by route 3.

Table 11 Relative weakness (EQ4)

Route	r_{ik}				R_i
	R.D.	Liq.	R.B.	Bridge	
1	1.000	1.000	0.355	1.000	3.355
2	0.919	0.765	0.290	0.730	2.704
3	0.716	0.509	1.000	0.792	3.017
4	0.742	0.985	0.903	0.856	3.486
5	0.708	0.809	0.919	0.856	3.292
6	0.649	0.770	0.774	0.945	3.138

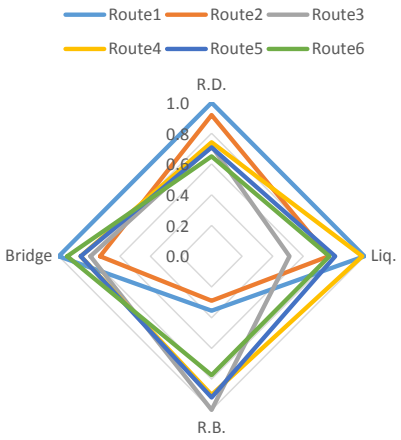

Fig. 13 Radar chart of relative weakness (EQ4)

4.2.5 Summary of prioritization

In order to prioritize transport route, we employed the suitability index I_i that is the inverse of R_i mentioned before. Namely, the index larger is, the higher the suitability is. Comparison of suitability index is shown in Fig. 14 with figures of indices.

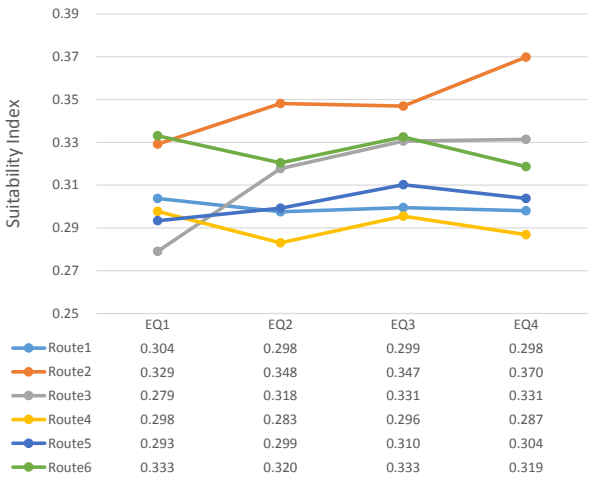

Fig. 14 Comparison of suitability index

From Fig. 2, it is apparent that the route 2 is the best selection since it gives largest or second largest suitability index regardless of scenario earthquakes. This is because route2 includes the highway so that the risk of road blockade is largely reduced. The route 6 is the second best selection because it is the shortest route.

5. Comparison of scenario earthquake

5.1 Procedure of comparison

Previous section describes the risk of each route. This section discuss the risk of each scenario earthquake. Instead of normalizing the maximum value, the relative risk of scenario earthquake is obtained.

5.2 Result of comparison

5.2.1 In case of route 1

The relative weaknesses for route 1 are summarized in Table 12 and Fig. 15. It is apparent that EQ1 gives the largest risk in each risk item, especially in liquefaction. This is because the route 1 passes through soft soil area, such as the coastal zone along the Tokyo bay or zone near to river, where liquefaction potential is high as shown in Fig.6.

Table 12 Relative weakness (Route 1)

EQ	r_{ik}				R_i
	R.D.	Liq.	R.B.	Bridge	
1	1.000	1.000	1.000	1.000	4.000
2	0.895	0.501	0.971	0.796	3.163
3	0.810	0.526	0.957	0.730	3.027
4	0.854	0.468	0.957	0.776	3.055

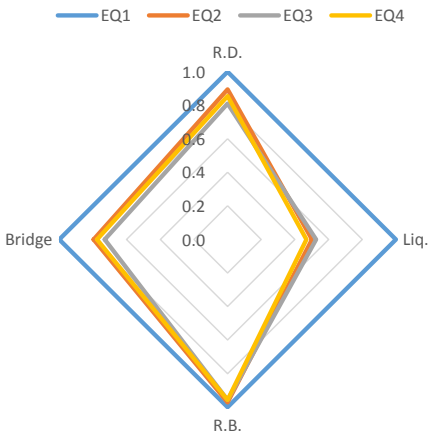

Fig. 15 Radar chart of relative weakness (Route 1)

5.2.2 In case of route 2

The relative weaknesses for route 2 are summarized in Table 13 and Fig. 16. It is apparent that EQ1 gives the largest risk in each risk item as stated in case of route 1. The tendency of the radar chart is similar to that for route 1.

Table 13 Relative weakness (Route 2)

EQ	r_{ik}				R_i
	R.D.	Liq.	R.B.	Bridge	
1	1.000	1.000	1.000	1.000	4.000
2	0.786	0.448	0.810	0.760	2.804
3	0.798	0.444	0.825	0.729	2.796
4	0.759	0.395	0.810	0.664	2.628

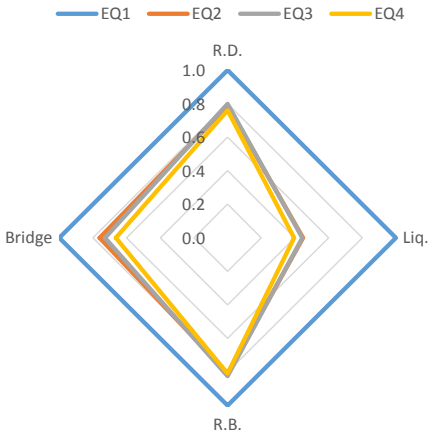

Fig. 16 Radar chart of relative weakness (Route 2)

5.2.3 In case of route 3

The relative weaknesses for route 3 are summarized in Table 14 and Fig. 17. It is apparent that EQ1 gives the largest risk in each risk item as stated in case of route 1. The tendency of the radar chart is similar to that for route 1.

Table 14 Relative weakness (Route 3)

EQ	r_{ik}				R_i
	R.D.	Liq.	R.B.	Bridge	
1	1.000	1.000	1.000	1.000	4.000
2	0.758	0.342	0.788	0.732	2.620
3	0.765	0.320	0.792	0.618	2.495
4	0.704	0.303	0.788	0.677	2.742

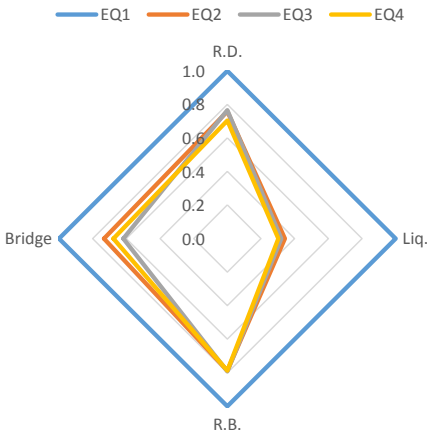

Fig. 17 Radar chart of relative weakness (Route 3)

5.2.4 In case of route 4

The relative weaknesses for route 4 are summarized in Table 15 and Fig. 18. It is apparent that EQ1 gives the largest risk in each risk item. Being different from previous cases, the relative risk of liquefaction in case of EQs 2, 3 and 4 are high. This is because the risk of liquefaction in case of EQ1 is small since route 4 passes through the zone where the liquefaction potential is low.

Table 15 Relative weakness (Route 4)

EQ	r_{ik}				R_i
	R.D.	Liq.	R.B.	Bridge	
1	1.000	1.000	1.000	1.000	4.000
2	0.870	0.620	0.816	0.759	3.065
3	0.795	0.597	0.840	0.677	2.909
4	0.799	0.611	0.792	0.732	2.934

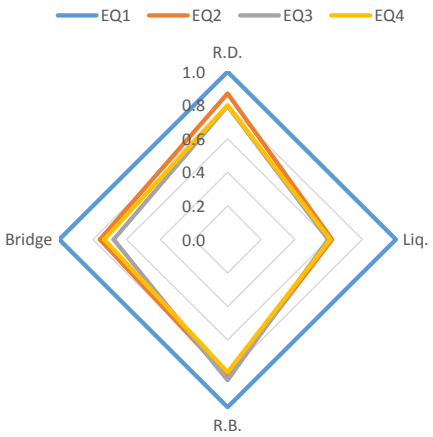

Fig. 18 Radar chart of relative weakness (Route 4)

5.2.5 In case of route 5

The relative weaknesses for route 5 are summarized in Table 16 and Fig. 19. It is apparent that EQ1 gives the largest risk in each risk item as stated in previous cases. The tendency of the radar chart is similar to that for route 4.

Table 16 Relative weakness (Route 5)

EQ	r_{ik}				R_i
	R.D.	Liq.	R.B.	Bridge	
1	1.000	1.000	1.000	1.000	4.000
2	0.864	0.505	0.813	0.759	2.911
3	0.796	0.487	0.842	0.677	2.802
4	0.775	0.505	0.804	0.732	2.816

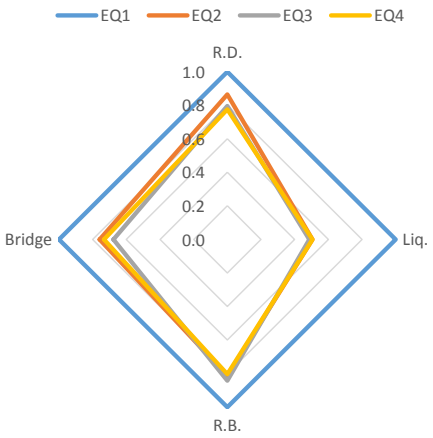

Fig. 19 Radar chart of relative weakness (Route 5)

5.2.6 In case of route 6

The relative weaknesses for route 6 are summarized in Table 17 and Fig. 20. It is apparent that EQ1 gives the largest risk in each risk item as stated in previous cases. The tendency of the radar chart is similar to that for route 4.

Table 17 Relative weakness (Route 6)

EQ	r_{ik}				R_i
	R.D.	Liq.	R.B.	Bridge	
1	1.000	1.000	1.000	1.000	4.000
2	0.858	0.568	0.818	0.832	3.706
3	0.772	0.571	0.818	0.754	2.915
4	0.799	0.568	0.796	0.832	2.995

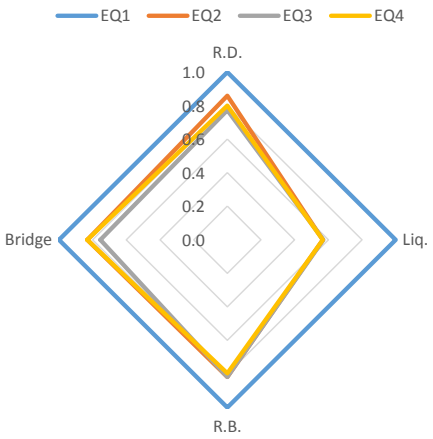

Fig. 20 Radar chart of relative weakness (Route 5)

6. Conclusions

In this paper, we evaluated the transport risk of six routes from Atsugi of Kanagawa prefecture to Shinagawa of Tokyo metropolitan for four scenario earthquakes. Four risk items, such as damage to road, liquefaction, load blockade and damage to road, were selected to grasp the risk.

It was illustrated that the suitable transport route can be selected by comparing the risk of each route. Also, the weak points or issues in each route were identified so that the proper counter measures can be selected against future disasters.

We employed the deterministic method to evaluate the transport risk, since the method can give us the detailed information on the risk, though the earthquake occurrence is probabilistic in reality. Therefore, it will necessary to conduct the probabilistic risk evaluation as the second step of this research.

References

1) Cabinet office, Government of Japan: Report on seismic fault models of M7 class earthquakes in metropolitan area and of M8 class earthquakes along Sagami trough, on intensity map and Tsunami height, and on others, 2013.

2) FUJIMOTO Kazuo and MIDORIKAWA Saburoh: Relationship between Average Shear-Wave Velocity and Site Amplification Inferred from Strong Motion Records at Nearby Station Pairs, *Journal of Japan Association for Earthquake Engineering*, Volume 6, Number 1, pp.11-22, 2006

3) HATA Akihito and KATAOKA Shojiro: Statistical Analysis of Damage to Highway Bridges Caused by the 2011 Off the Pacific Coast of Tohoku Earthquake, Journal of Japan Society of Civil Engineers A1, Volume 72, Number 4, pp.I_676-I_690, 2016

4) MATSUOKA Masashi, WAKAMATSU Kazue

and HASHIMOTO Mitsufumi: Liquefaction Potential Estimation Based on the 7.5-arc-second Japan Engineering Geomorphologic Classification Map, *Journal of Japan Association for Earthquake Engineering*, Volume 11, Number 2, pp.20-39, 2011

5) TORISAWA Kazuaki, YOSHIDA Satoshi and SADOHARA Satoru: A Study on Road Network Damage Prediction and its Influence Estimation to Business Continuity of Supply Chain, *Journal of Japan Association for Earthquake Engineering*, Volume 14, Number 2, pp.84-103, 2014

6) Wakamatsu, K. and Matsuoka, M.: Nationwide 7.5-Arc-Second Japan Engineering Geomorphologic Classification Map and Vs30 Zoning, *Journal of Disaster Research*, Vol.8 No.5, pp.904-911, 2013